Available online www.ejaet.com

European Journal of Advances in Engineering and Technology, 2017, 4 (1): 56-63

Research Article ISSN: 2394 - 658X

Effects of Hall Current and Chemical Reaction on MHD Flow Through Porous Medium Past an Oscillating Inclined Plate with Variable Temperature and Mass Diffusion

US Rajput and Gaurav Kumar

Department of Mathematics and Astronomy, University of Lucknow, UP, India
rajputgauravlko@gmail.com

ABSTRACT

The present study is carried out to examine the effects of Hall current and chemical reaction on unsteady MHD flow through porous medium past an oscillating inclined plate with variable wall temperature and mass diffusion. The fluid taken is electrically conducting. The Governing equations involved in the present analysis are solved by the Laplace-transform technique. The velocity profile is discussed with the help of graphs drawn for different parameters. The numerical values of skin-friction and Sherwood number have been tabulated.

Key words: MHD flow, Chemical reaction, oscillating inclined plate, Hall current

INTRODUCTION

The influence of magnetic field on viscous, incompressible and electrically conducting fluid is of great importance in many applications such as magnetic material processing, glass manufacturing control processes and purification of crude oil. Hall current and chemical reaction effects on MHD flow is also significant in many cases. Oscillatory magneto hydrodynamic flow past a flat plate with Hall effect was investigated by Datta and Jana [7]. Chen [3] has examined heat and mass transfer in MHD flow by natural convection from a permeable inclined surface with variable wall temperature and concentration. Unsteady two dimensional flow of a radiating and chemically reacting MHD fluid with time dependent suction was discussed by Prakash and Ogulu [8]. Abdelkhalek [6] has worked on heat and mass transfer in MHD free convection from a moving permeable vertical surface. Effect of variable fluid properties on the natural convective boundary layer flow of a nano fluid past a vertical plate was investigated by Afify and Bazid [1]. Dash et al. [4] have considered chemical reaction effect on MHD free convective surface over a moving vertical plate through porous medium. Kumar et al. [5] have proposed chemical reaction effect on MHD viscous flow past an impulsively started infinite vertical plate. Seshaiah and Verma [2] have analyzed chemical reaction effect on MHD free convective flow through porous medium with constant suction and heat flux. Unsteady MHD flow in porous media past over exponentially accelerated inclined plate with variable wall temperature and mass transfer along with Hall current was analyzed by us [9]. In this paper we are considering effects of Hall current and chemical reaction on unsteady MHD flow through porous medium past an oscillating inclined plate with variable temperature and mass diffusion. The results are shown with the help of graphs and table.

MATHEMATICAL ANALYSIS

MHD flow past an electrically non conducting plate inclined at an angle α from vertical is considered. The Geometrical model of the flow problem is shown in Fig. 1. The x axis is taken along the plane and z normal to it. A transverse magnetic field B_0 of uniform strength is applied on the flow. Initially, it has been considered that the plate as well as the fluid is at the same temperature T_∞. The species concentration in the fluid is taken as C_∞. At time t > 0, the plate starts oscillating in its own plane with frequency ω, and temperature of the plate is raised to T_w. The concentration C near the plate is raised linearly with respect to time. The flow modal is as under:

$$\frac{\partial u}{\partial t} = \upsilon \frac{\partial^2 u}{\partial z^2} + g\beta Cos\alpha (T - T_\infty) + g\beta^* Cos\alpha (C - C_\infty) - \frac{\sigma B_0^2 (u + mv)}{\rho (1 + m^2)} - \frac{\upsilon u}{K}. \quad (1)$$

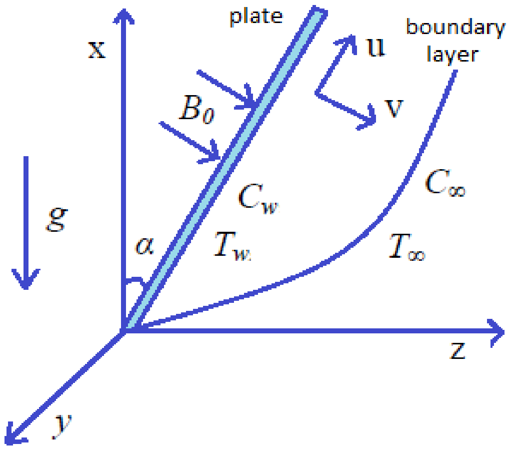

Fig. 1Physical Model

$$\frac{\partial v}{\partial t}=\upsilon\frac{\partial^2 v}{\partial z^2}+\frac{\sigma B_0^2(mu-v)}{\rho(1+m^2)}-\frac{\upsilon v}{K}. \quad (2)$$

$$\frac{\partial C}{\partial t}=D\frac{\partial^2 C}{\partial z^2}-K_c(C-C_\infty). \quad (3)$$

$$\rho C_p\frac{\partial T}{\partial t}=k\frac{\partial^2 T}{\partial z^2}. \quad (4)$$

The boundary conditions for the flow are as under:

$$\left.\begin{array}{l} t\le 0: u=0, v=0, T=T_\infty, C=C_\infty, \text{ for every z,} \\ t>0: u=u_0 Cos\omega t, v=0, T=T_\infty+(T_w-T_\infty)A_0, C=C_\infty+(C_w-C_\infty)A_0, \text{ at z=0} \\ u\to 0, v\to 0, T\to T_\infty, C\to C_\infty \text{ as } z\to 0. \end{array}\right\} \quad (5)$$

Here u is the primary velocity, v - the secondary velocity, g- the acceleration due to gravity, β- volumetric coefficient of thermal expansion, t- time, m is the Hall parameter, K- the permeability parameter, T- temperature of the fluid, β^*- volumetric coefficient of concentration expansion, C- species concentration in the fluid, ϑ- the kinematic viscosity, ρ- the density, C_p- the specific heat at constant pressure, k- thermal conductivity of the fluid, D- the mass diffusion coefficient, T_w- temperature of the plate at z= 0,C_w - species concentration at the plate z= 0, B_0- the uniform magnetic field, K_C-chemical reaction, σ- electrical conductivity

The following non-dimensional quantities are introduced to transform equations (1), (2), (3) and (4) into dimensionless form:

$$\left.\begin{array}{l} \bar{z}=\frac{zu_0}{\upsilon}, \bar{u}=\frac{u}{u_0}, \bar{v}=\frac{v}{u_0}, \theta=\frac{(T-T_\infty)}{(T_w-T_\infty)}, S_c=\frac{\upsilon}{D}, \mu=\rho\upsilon, M=\frac{\sigma B_0^2\upsilon}{\rho u_0^2}, \bar{C}=\frac{(C-C_\infty)}{(C_w-C_\infty)}, \\ G_r=\frac{g\beta\upsilon(T_w-T_\infty)}{u_0^3}, G_m=\frac{g\beta^*\upsilon(C_w-C_\infty)}{u_0^3}, \bar{t}=\frac{tu_0^2}{\upsilon}, P_r=\frac{\mu c_p}{k}, \bar{K}=\frac{u_0}{\upsilon^2}K, \bar{\omega}=\frac{\omega\upsilon}{u_0^2}. \end{array}\right\} \quad (6)$$

The symbols in dimensionless form are as under: $\bar{u}$ is the Primary velocity, $\bar{v}$ - the secondary velocity, $\bar{t}$ - time, θ- the temperature, $\bar{C}$ - the concentration, $\bar{K}$ - the permeability parameter, G_r- thermal Grashof number, G_m- mass Grashof number, K_0 -chemical reaction parameter, μ - the coefficient of viscosity, P_r- the Prandtl number, S_c- the Schmidt number, M- the magnetic parameter.

Thus the model becomes

$$\frac{\partial\bar{u}}{\partial\bar{t}}=\frac{\partial^2\bar{u}}{\partial\bar{z}^2}+G_r Cos\alpha\,\theta+G_m Cos\alpha\,\bar{C}-\frac{M(\bar{u}+m\bar{v})}{(1+m^2)}-\frac{1}{\bar{K}}\bar{u}. \quad (7)$$

$$\frac{\partial\bar{v}}{\partial\bar{t}}=\frac{\partial^2\bar{u}}{\partial\bar{z}^2}+\frac{M(m\bar{u}-\bar{v})}{(1+m^2)}-\frac{1}{\bar{K}}\bar{v}. \quad (8)$$

$$\frac{\partial\bar{C}}{\partial\bar{t}}=\frac{1}{S_c}\frac{\partial^2\bar{C}}{\partial\bar{z}^2}-K_0\bar{C}. \quad (9)$$

$$\frac{\partial\theta}{\partial\bar{t}}=\frac{1}{P_r}\frac{\partial^2\theta}{\partial\bar{z}^2}. \quad (10)$$

The boundary conditions (5) become:

$$\left.\begin{array}{l} \bar{t}\le 0: \bar{u}=0, \bar{v}=0, \theta=0, \bar{C}=0, \text{ for every } \bar{z} \\ \bar{t}>0: \bar{u}=Cos\bar{\omega}\bar{t}, \bar{v}=0, \theta=\bar{t}, \bar{C}=\bar{t}, \text{ at } \bar{z}=0, \\ \bar{u}\to 0, \bar{v}\to 0, \theta\to 0, \bar{C}\to 0 \text{ as } \bar{z}\to\infty. \end{array}\right\} \quad (11)$$

Dropping bars in the above equations, we get

$$\frac{\partial u}{\partial t}=\frac{\partial^2 u}{\partial z^2}+G_r Cos\alpha\,\theta+G_m Cos\alpha\, C-\frac{M(u+mv)}{(1+m^2)}-\frac{1}{K}u. \quad (12)$$

$$\frac{\partial v}{\partial t}=\frac{\partial^2 v}{\partial z^2}+\frac{M(mu-v)}{(1+m^2)}-\frac{1}{K}v. \quad (13)$$

$$\frac{\partial C}{\partial t}=\frac{1}{S_c}\frac{\partial^2 C}{\partial z^2}-K_0 C. \quad (14)$$

$$\frac{\partial \theta}{\partial t}=\frac{1}{P_r}\frac{\partial^2 \theta}{\partial z^2}. \quad (15)$$

The boundary conditions become:

$$\left.\begin{array}{l} t\le 0: u=0, v=0, \theta=0, C=0, \text{ for every z,}\\ t>0: u=Cos\omega t, v=0, \theta=t, C=t, \text{ at z=0,}\\ u\to 0, v\to 0, \theta\to 0, C\to 0, \text{ as } z\to\infty. \end{array}\right\} \quad (16)$$

Writing the equations (15) and (16) in combined form (using $q= u + i\, v$)

$$\frac{\partial q}{\partial t}=\frac{\partial^2 q}{\partial z^2}+G_r Cos\alpha\,\theta+G_m Cos\alpha C-qa. \quad (17)$$

$$\frac{\partial C}{\partial t}=\frac{1}{S_c}\frac{\partial^2 C}{\partial z^2}-K_0 C. \quad (18)$$

$$\frac{\partial \theta}{\partial t}=\frac{1}{P_r}\frac{\partial^2 \theta}{\partial z^2}. \quad (19)$$

The boundary conditions (16) are reduced to

$$\left.\begin{array}{l} t\le 0: q=0, \theta=0, C=0, \text{ for every z,}\\ t>0: q=Cos\omega t, \theta=t, C=t, \text{ at z=0}\\ q\to 0, \theta\to 0, C\to 0, \text{ as } z\to\infty . \end{array}\right\} \quad (20)$$

The dimensionless governing equations (17) to (19), subject to the boundary conditions (20), are solved by the usual Laplace - transform technique.

The solution obtained is as under: $\theta=t\left\{(1+\frac{z^2 P_r}{2t})erfc[\frac{\sqrt{P_r}}{2\sqrt{t}}]-\frac{z\sqrt{P_r}}{\sqrt{\pi}\sqrt{t}}e^{-\frac{z^2}{4t}P_r}\right\}.$

$$C=\frac{e^{-z\sqrt{S_c K_0}}}{4\sqrt{K_0}}\left\{erfc[\frac{z\sqrt{S_c}-2t\sqrt{K_0}}{2\sqrt{t}}](-z\sqrt{S_c}+2t\sqrt{K_0})+e^{2z\sqrt{S_c K_0}}erfc[\frac{z\sqrt{S_c}+2t\sqrt{K_0}}{2\sqrt{t}}](z\sqrt{S_c}+2t\sqrt{K_0})\right\}.$$

$$q=\frac{e^{-it\omega}A_{15}}{4}+\frac{G_r Cos\alpha}{4a^2}\left[zA_{11}+2e^{-\sqrt{a}z}A_2P_r+2A_{14}A_4(1-P_r)\right]+\frac{G_m Cos\alpha}{4(a-K_0S_c)^2}[\,zA_{11}+2A_{13}A_5(1-S_c)$$

$$+2e^{-\sqrt{a}z}A_2S_c(1-tK_0)-\frac{ze^{-\sqrt{a}z}A_3K_0S_c}{\sqrt{a}}\,]\;+\;\frac{G_r Cos\alpha}{2a^2\sqrt{\pi}}[2zae^{\frac{-z^2P_r}{4t}}\sqrt{tP_r}+\sqrt{\pi}A_{14}(A_6+A_7P_r)+$$

$$\sqrt{\pi}A_{12}(az^2P_r-2+2at+2P_r)]+\frac{G_m Cos\alpha}{4\sqrt{\pi}(a-K_0S_c)^2}[\frac{e^{-\sqrt{K_0S_c}}\sqrt{\pi}A_9\sqrt{S_c}}{2\sqrt{K_0}}(S_cK_0-az)+A_{13}\sqrt{\pi}A_{10}$$

$$(S_c-1)+e^{-\sqrt{K_0S_c}}\sqrt{\pi}A_8(1-at-S_c+tK_0S_c)]$$

The expressions for the constants involved in the above equations are given in the appendix.

Skin Friction

The dimensionless skin friction at the plate z=0 is obtained by

$$\left(\frac{dq}{dz}\right)_{z=0}=\tau_x+i\tau_y\,.$$

The numerical values of τ_x and τ_y, for different parameters are given in table-1.

Table -1 Skin Friction for Different Parameters (α and ωt are in degrees)

A	*M*	*m*	*Pr*	*Sc*	*Gm*	*Gr*	K_0	*t*	*K*	ωt	τ_x	τ_y
15	2	0.5	0.71	2.01	100	10	1	0.2	0.2	30	07.30783	03.37140
30	2	0.5	0.71	2.01	100	10	1	0.2	0.2	30	06.08396	03.05818
45	2	0.5	0.71	2.01	100	10	1	0.2	0.2	30	04.13708	02.55991
60	2	0.5	0.71	2.01	100	10	1	0.2	0.2	30	01.59984	01.91056
30	1	0.5	0.71	2.01	100	10	1	0.2	0.2	30	08.48051	02.16472
30	3	0.5	0.71	2.01	100	10	1	0.2	0.2	30	04.28780	03.39279
30	2	2.0	0.71	2.01	100	10	1	0.2	0.2	30	08.33943	03.53606
30	2	3.0	0.71	2.01	100	10	1	0.2	0.2	30	09.62902	03.12749
30	2	0.5	7.00	2.01	100	10	1	0.2	0.2	30	05.95327	03.05462
30	2	0.5	0.71	3.00	100	10	1	0.2	0.2	30	13.53750	08.41395
30	2	0.5	0.71	4.00	100	10	1	0.2	0.2	30	27.47610	28.45430
30	2	0.5	0.71	2.01	010	10	1	0.2	0.2	30	-03.21156	00.61885
30	2	0.5	0.71	2.01	050	10	1	0.2	0.2	30	00.91978	01.70300
30	2	0.5	0.71	2.01	100	50	1	0.2	0.2	30	07.20873	03.07788
30	2	0.5	0.71	2.01	100	10	2	0.2	0.2	30	28.15360	29.23390
30	2	0.5	0.71	2.01	100	10	1	0.3	0.2	30	12.03590	04.46902
30	2	0.5	0.71	2.01	100	10	1	0.4	0.2	30	18.12800	05.88362
30	2	0.5	0.71	2.01	100	10	1	0.2	1.0	30	-40.28400	29.14080
30	2	0.5	0.71	2.01	100	10	1	0.2	0.2	45	06.72416	03.03956
30	2	0.5	0.71	2.01	100	10	1	0.2	0.2	90	09.41131	02.95329

Table -2 Sherwood Number for Different Parameters

K_o	S_c	*T*	S_h
1	2.01	0.2	-0.762200
5	2.01	0.2	-0.933049
10	2.01	0.2	-1.118240
1	3.00	0.2	-0.931175
1	4.00	0.2	-1.075230
1	2.01	0.3	-0.961323
1	2.01	0.4	-1.141570

Sherwood Number

The dimensionless Sherwood number at the plate z=0 is given by

$$S_h = \left(\frac{\partial C}{\partial z}\right)_{z=0} = erfc[-\sqrt{tK_0}](-\frac{1}{4\sqrt{K_0}}\sqrt{S_c} - \frac{t\sqrt{S_c K_0}}{2}) + \sqrt{S_c}\,erfc[\sqrt{tK_0}](\frac{1}{4\sqrt{K_0}} + t\sqrt{K_0}) - \frac{e^{-tK_0}\sqrt{tS_c K_0}}{\sqrt{\pi K_0}}$$

The numerical values of Sherwood number for different parameters are given in table-2.

RESULT AND DISCUSSIONS

The velocity profile for different parameters like, thermal Grashof number (*Gr*), magnetic field parameter (*M*), Hall parameter (*m*), Prandtl number (*Pr*), chemical reaction parameter(K_0), acceleration parameter (*b*) and time (t) is shown in Figs. 2 to 23. It is observed from Figs. 2 and 13 that the primary and secondary velocities of fluid decrease when the angle of inclination (α) is increased. It is observed from Fig. 3 and 14, when the mass Grashof number *Gm* is increased then the velocities are increased. From Figs. 4 and 15 it is deduced that velocities increases with thermal Grashof number *Gr*. If Hall current parameter *m* is increased then u increases, while *v* gets decreased (Figs. 5 and 16). Also, it is observed from Figs. 6 and 17 that the effect of increasing values of the parameter *M* results in decreasing u and increasing v. It is deduced that when chemical reaction parameter K_0 is increased then the velocities are decreased (Figs. 7 and 18). It is deduced that when permeability parameter is increased then the velocities are increased (Figs. 8 and 19). It is observed from Figs. 9 and 20 that phase angle ωt is increases then the velocities are decreased. It is noticed that velocities decrease when Prandtl number and Schmidt number are increased (Figs. 10, 11, 21 and 22). Further, from Figs. 12 and 23, it is observed that velocities increase with time.

Skin friction is given in table -1. The value of τ_x increases with the thermal Grashof Number, the mass Grashof number, Hall current parameter, chemical reaction parameter, phase angle, Schmidt number and time, and it decreases with increase in the angle of inclination of plate, permeability parameter, the magnetic field parameter and Prandtl number, and Similar effect is observed with τ_y, except permeability parameter, Hall parameter, the magnetic field parameter and phase angle, in which case τ_y increases with permeability parameter, the magnetic field parameter, and decreases with Hall parameter and phase angle.

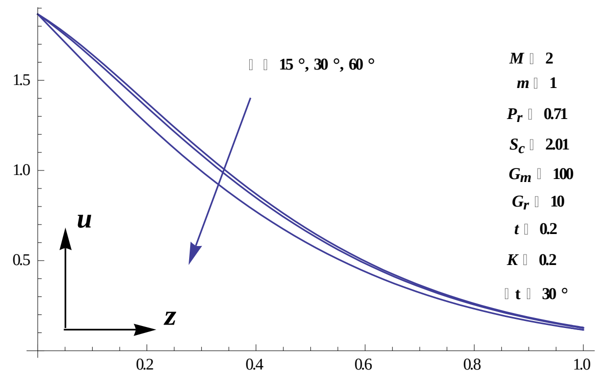

Fig. 2 Velocity *u* for different values of *α*

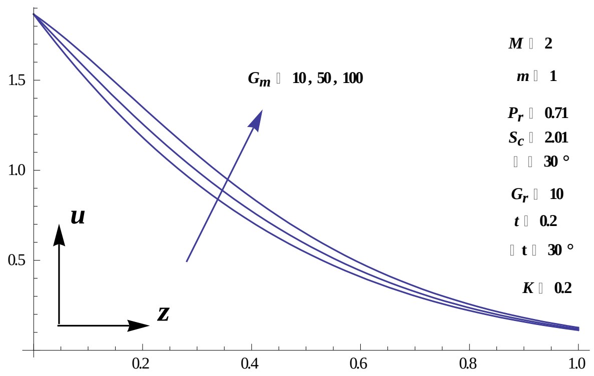

Fig. 3 Velocity *u* for different values of *Gm*

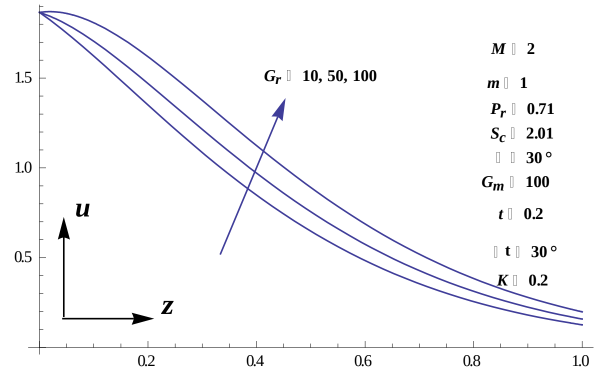

Fig. 4 Velocity *u* for different values of *Gr*

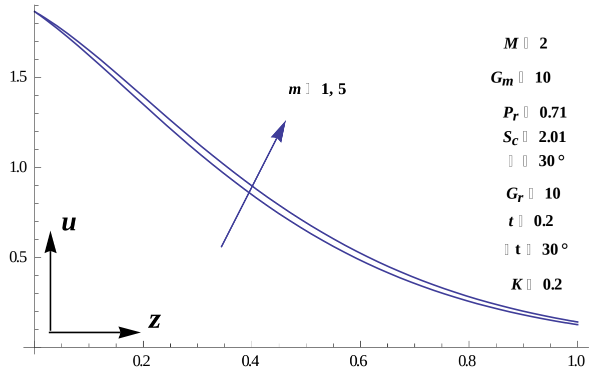

Fig. 5 Velocity *u* for different values of *m*

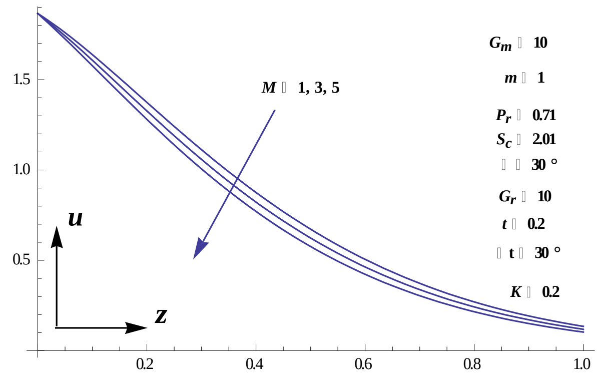

Fig. 6 Velocity *u* for different values of *M*

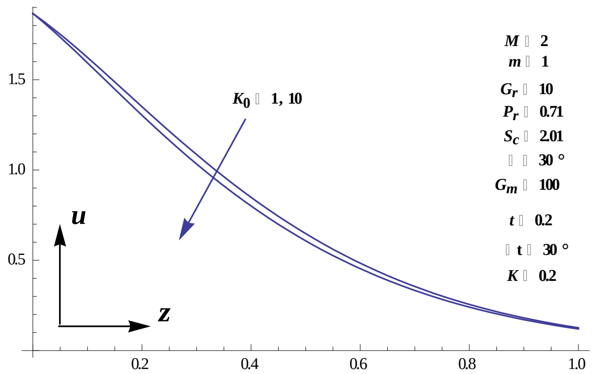

Fig. 7 Velocity *u* for different values of *Ko*

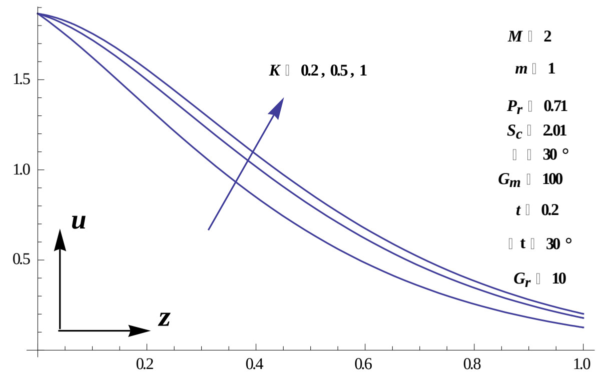

Fig. 8 Velocity *u* for different values of *K*

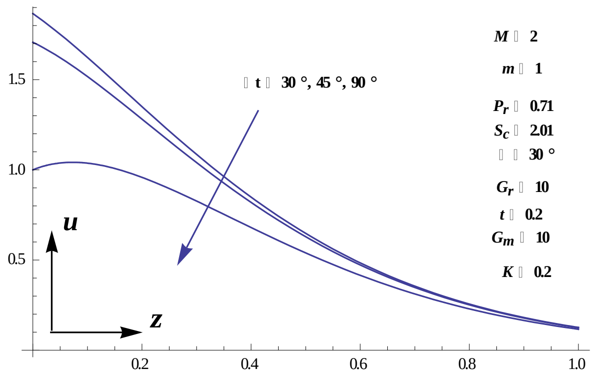

Fig. 9 Velocity *u* for different values of *ωt*

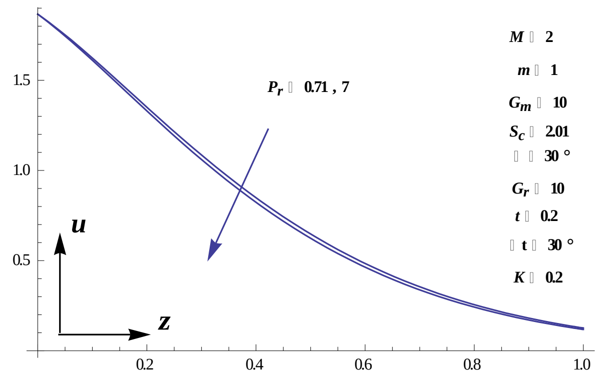

Fig. 10 Velocity *u* for different values of *Pr*

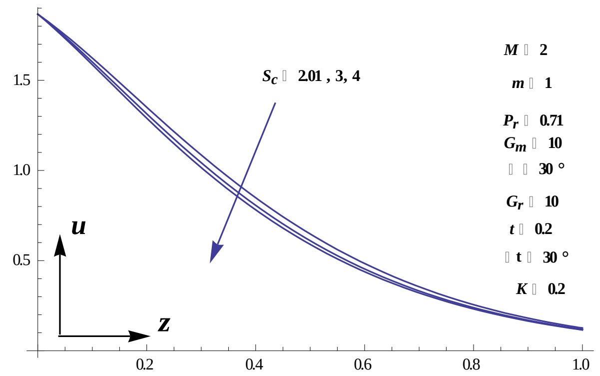

Fig. 11 Velocity *u* for different values of *Sc*

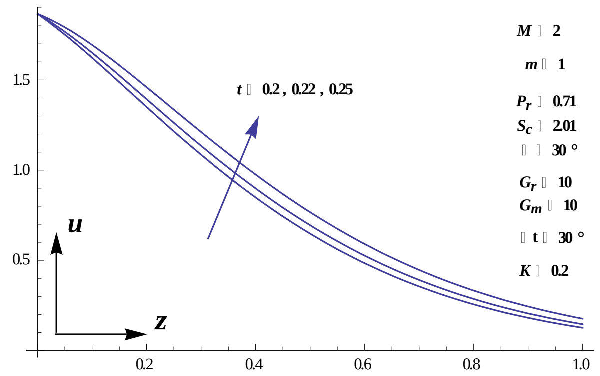

Fig. 12 Velocity *u* for different values of *t*

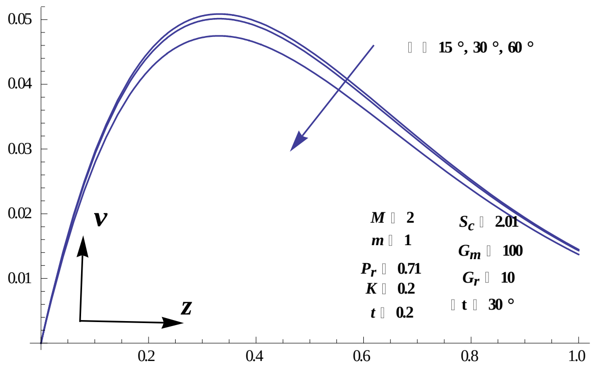

Fig. 13 Velocity *v* for different values of α

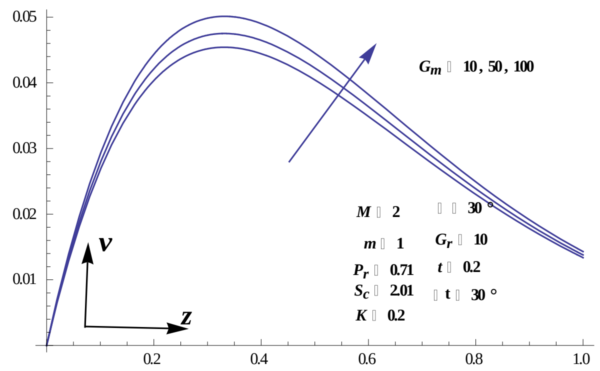

Fig. 14 Velocity *v* for different values of *Gm*

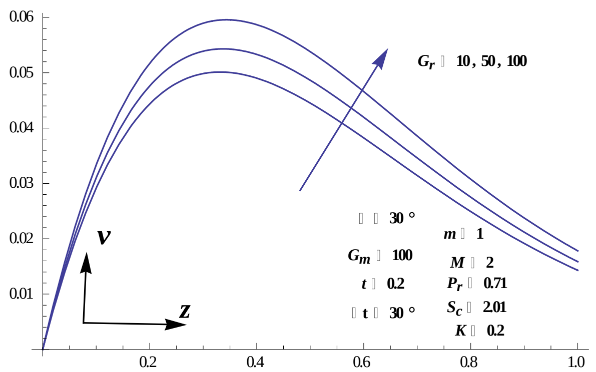

Fig. 15 velocity *v* for different values of *Gr*

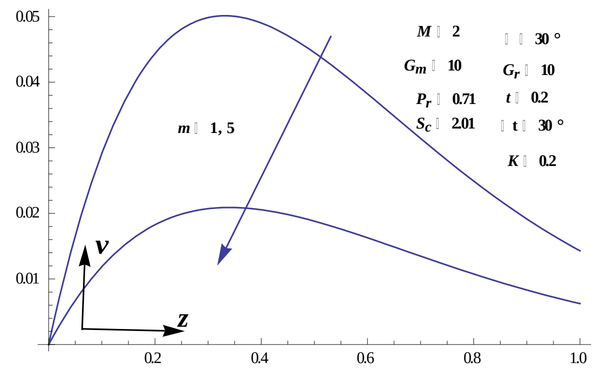

Fig. 16 Velocity *v* for different values of *m*

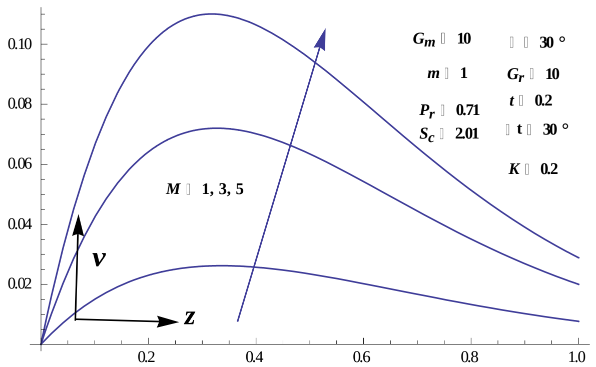

Fig. 17 Velocity *v* for different values of *M*

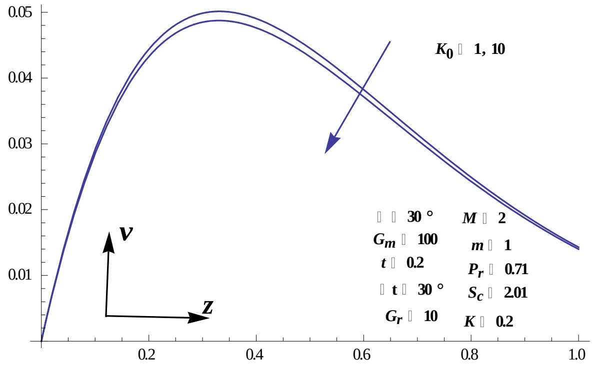

Fig. 18 Velocity *v* for different values of *Ko*

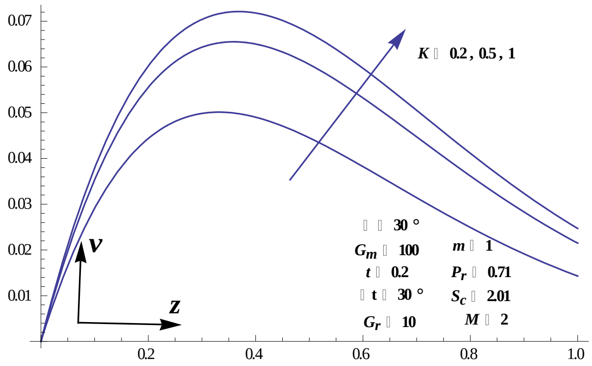

Fig. 19 Velocity *v* for different values of *K*

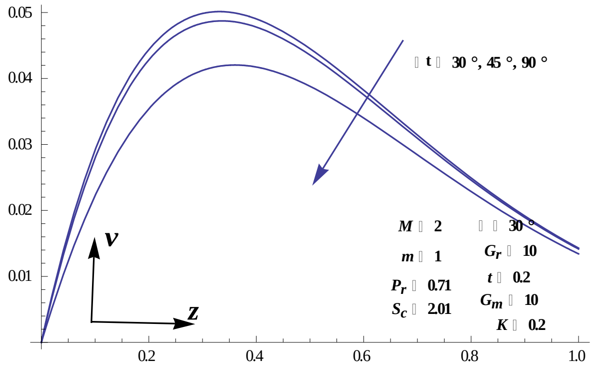

Fig. 20 Velocity *v* for different values of *ωt*

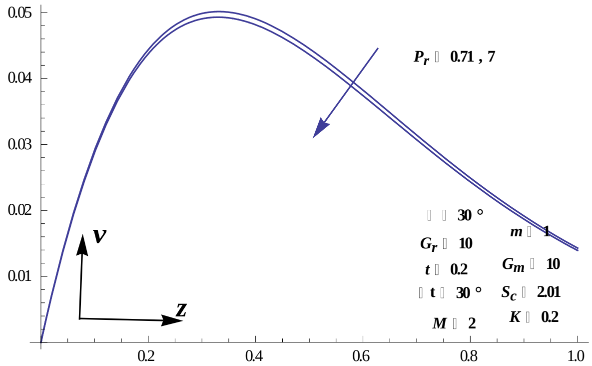

Fig. 21 Velocity *v* for different values of *Pr*

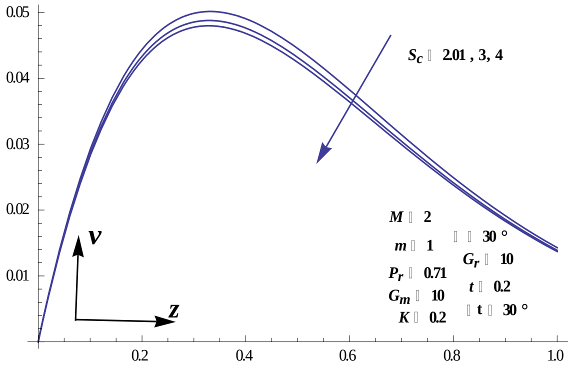

Fig. 22 Velocity *v* for different values of *Sc*

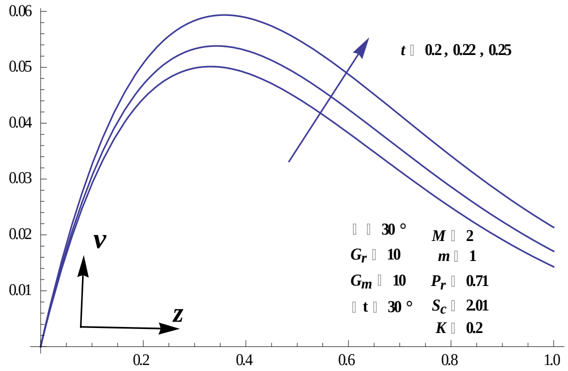

Fig. 23 Velocity *v* for different values of *t*

CONCLUSION

The conclusions of the study are as follows:

- Primary velocity increases with the increase in *Gr*, *Gm*, *K*, *Pr*, *m* and *t*.
- Primary velocity decreases with *α*, *M*, K_0, *ωt*, *Pr* and *Sc*.
- Secondary velocity increases with the increase in *Gr*, *Gm*, *K*, *M* and *t*.
- Secondary velocity decreases with *α*, *m*, K_0, *ωt*, *Pr* and *Sc*.
- τ_x increases with the increase in *Gr*, *Gm*, K_0, *m*, *Sc*, *ωt* and *t*, and it decreases with *α, b*, *M*, *K* and *Pr*.
- τ_y increases with the increase in *Gr*, *Gm*, *b*, *K*, K_0, *M*, *Sc* and *t*, and it decreases with *α, m*, *ωt* and *Pr*.

REFERENCES

[1] AA Afify and MAA Bazid, Effects of Variable Fluid Properties on the Natural Convective Boundary Layer Flow of a Nanofluid Past a Vertical Plate: Numerical Study, *Journal of Computational and Theoretical Nanoscience*, **2014**, 11, 210–218.

[2] B Seshaiah and SVK Verma, Chemical Reaction Effects on MHD Free Convective Flow through Porous Medium with Constant Suction and Heat Flux, *International Journal of Applied Sciences*, **2016**, 3(3), 340 – 355.
[3] CH Chen, Heat and Mass Transfer in MHD Flow by Natural Convection from a Permeable Inclined Surface with Variable Wall Temperature and Concentration, *Acta Mechanica*, **2004**, 17(2), 219- 235.
[4] GC Dash, RS Tripathi, SR Mishra and S Baag, Chemical Reaction Effect on MHD Free Convective Surface over a Moving Vertical Plate through Porous Medium, *Alexandria Engineering Journal*, **2015**, 54 (3), 1-7.
[5] JG Kumar, PS Reddy and RVS Prasad, Chemical Reaction Effects on MHD Viscous Flow Past an Impulsively Started Infinite Vertical Plate, *International Journal of Mathematics and Computer Research*, **2016**, 4(7), 1526-1540.
[6] MM Abdelkhalek, Heat and Mass Transfer in MHD Free Convection from a Moving Permeable Vertical Surface by a Perturbation Technique, *Communications in Nonlinear Science and Numerical Simulation*, **2009**, 14, 2091-2102.
[7] N Datta and RN Jana, Oscillatory Magneto Hydrodynamic Flow Past a Flat Plate Will Hall Effects, *Journal of the Physical Society of Japan*, **1976**, 40, 14-69.
[8] Prakash and J Ogulu A, Unsteady Two-Dimensional Flow of a Radiating and Chemically Reacting MHD Fluid with Time Dependent Suction, *Indian Journal of Pure and Applied Physics*, **2006**, 44, 805-810.
[9] US Rajput and Kumar Gaurav, Unsteady MHD Flow in Porous Media Past Over Exponentially Accelerated Inclined Plate with Variable Wall Temperature and Mass Transfer along with Hall Current, *International Journal of Engineering, Science and Technology*, **2016**, 8(2), 1-10.

Appendix

$$a=\frac{M(1-im)}{1+m^2}+\frac{1}{K},\ A_1=1+A_{16}+e^{2\sqrt{a}z}(1-A_{17}),\ A_2=-A_1,\ A_3=A_{16}-A_1,\ A_4=-1+A_{22}+A_{18}(A_{23}-1),$$

$$A_5=-1+A_{24}+A_{19}(A_{25}-1),\ A_6=-1-A_{26}+A_{18}(A_{27}-1),\ A_7=-A_6,\ A_8=-1-A_{20}+A_{30}(A_{21}-1),$$

$$A_9=A_8+2(A_{20}+1),\ A_{10}=-1-A_{28}+A_{19}(A_{29}-1),\ A_{11}=\frac{e^{-\sqrt{a}z}}{z}(2A_1+2atA_2+\sqrt{a}A_3),\ A_{12}=-1+erf\left[\frac{z\sqrt{P_r}}{2\sqrt{t}}\right],$$

$$A_{13}=e^{\frac{at}{-1+S_c}-z\sqrt{\frac{(a-K_0)S_c}{-1+S_c}}-\frac{tK_0S_c}{-1+S_c}},\ A_{14}=e^{\frac{at}{-1+P_r}-z\sqrt{\frac{(a)P_r}{-1+P_r}}},\ A_{15}=A_{31}+A_{32}-e^{-z\sqrt{a+i\omega}}A_{33}-e^{-z\sqrt{a+i\omega}+2it\omega}A_{34},$$

$$A_{16}=erf[\frac{2\sqrt{at}-z}{2\sqrt{t}}],\ A_{17}=erf[\frac{2\sqrt{at}+z}{2\sqrt{t}}],\ A_{18}=e^{-2z\sqrt{\frac{aP_r}{-1+P_r}}},\ A_{19}=e^{-2z\sqrt{\frac{(a-K_0)S_c}{-1+S_c}}},\ A_{20}=erf\left[\sqrt{tK_0}-\frac{z\sqrt{S_c}}{2\sqrt{t}}\right],$$

$$A_{21}=erf\left[\sqrt{tK_0}+\frac{z\sqrt{S_c}}{2\sqrt{t}}\right],\ A_{22}=erf[\frac{z-2t\sqrt{\frac{aP_r}{-1+P_r}}}{2t}],\ A_{23}=erf[\frac{z+2t\sqrt{\frac{aP_r}{-1+P_r}}}{2t}],\ A_0=\frac{u_0^2t}{\upsilon}$$

$$A_{24}=erf[\frac{z-2t\sqrt{\frac{(a-K_0)S_c}{-1+S_c}}}{2t}],\ A_{25}=erf[\frac{z+2t\sqrt{\frac{(a-K_0)S_c}{-1+S_c}}}{2t}],\ A_{26}=erf[\frac{2t\sqrt{\frac{a}{-1+P_r}}-z\sqrt{P_r}}{2\sqrt{t}}],$$

$$A_{27}=erf[\frac{2t\sqrt{\frac{a}{-1+P_r}}+z\sqrt{P_r}}{2\sqrt{t}}],\ A_{28}=erf[\sqrt{t}\sqrt{\frac{(a-K_0)}{-1+S_c}}-\frac{zS_c}{2\sqrt{t}}],\ A_{29}=erf[\sqrt{t}\sqrt{\frac{(a-K_0)}{-1+S_c}}+\frac{zS_c}{2\sqrt{t}}],$$

$$A_{30}=erf[e^{2z\sqrt{K_0\sqrt{S_c}}}],\ A_{31}=e^{-z\sqrt{a+i\omega}}+e^{-z\sqrt{a-i\omega}},\ A_{32}=e^{-z\sqrt{a+i\omega}+2it\omega}+e^{z\sqrt{a-i\omega}+2it\omega},$$

$$A_{33}=erf\left[\frac{z-2t\sqrt{a-i\omega}}{2\sqrt{t}}\right]+erf\left[\frac{z+2t\sqrt{a-i\omega}}{2\sqrt{t}}\right],\ A_{34}=erf\left[\frac{z-2t\sqrt{a+i\omega}}{2\sqrt{t}}\right]+erf\left[\frac{z+2t\sqrt{a+i\omega}}{2\sqrt{t}}\right]$$